Sound absorption of a rib-stiffened plate covered by anechoic coatings

Xinyi Fu, Zhongkun Jin, Yao Yin, and Bilong Liu[a)]
Key Laboratory of Noise and Vibration Research, Institute of Acoustics, Chinese Academy of Sciences, 100190 Beijing, People's Republic of China

(Received 10 May 2014; revised 10 February 2015; accepted 18 February 2015)

Underwater vehicles are often equipped with anechoic coatings to absorb the sound waves of active sonar and attenuate the noise emitted from the vessels. Rubber layers with periodically distributed air cavities are widely used as anechoic coatings. In this paper, the sound absorption of anechoic coatings embedded with doubly periodic cavities and backed with periodically rib-stiffened plates is investigated using a finite element method (FEM) with Bloch-periodic boundary conditions. Numerical results given by the FEM are compared with those of a simplified transfer impedance approach to explain the shifting of the main absorption peak. Further a simplified FEM approach, which reduces calculation time significantly and maintains the reasonable accuracy, is proposed for a comparison. The results indicate that the plate and the ribs can have significant impacts on the absorption performance of anechoic coatings, especially at low frequencies.
 [http://dx.doi.org/10.1121/1.4913782]

[LH] Pages: 1551–1556

I. INTRODUCTION

Underwater vehicles are often equipped with anechoic coatings to absorb the incident sound from active sonar and attenuate the self-noise. Rubber layers with periodically distributed air-filled cavities are widely used as anechoic coatings. During the past few decades, many mathematical models have been developed to study the sound absorptive performance of anechoic coatings. In general, these mathematical models can be classified as analytical and numerical models. Analytical approaches typically include transfer matrix method,[1] effective medium model,[2–5] and cavity resonances model.[6–9] Compared to an analytical approach, a numerical approach like finite element method (FEM) is more flexible in dealing with complex structures. The FEM combined with Bloch's theorem was previously introduced by Hennion[10,11] to investigate the sound reflection and insulation characteristics of anechoic coatings containing doubly periodic cavities. Under Bloch periodic boundary conditions, only a unit cell of the doubly periodic structure has to be modeled; this makes the computation of infinite structure feasible.

In practice, the hull of vehicle (the structure underneath the anechoic coatings) has a significant effect on sound absorptive performance, especially at low frequencies. Therefore it is reasonable to include the dynamics of the hull structure in the modeling.[12] A typical hull structure consists of periodically rib-stiffened plates. Because the space between two ribs is much larger than the space between two cavities in anechoic coatings, to include the effect of ribs, the unit cell to be meshed must be able to cover one period of rib space, and this results in a large model and time-consuming computation. Hull and Welch[13] recently developed an analytical model to investigate the vibro-acoustic response of a fluid-loaded anechoic coating affixed to a rib-stiffened plate. The similar problem was also investigated by Remillieux and Burdisso[14] using finite element analysis, while their analysis was limited in two dimensions. Their results were also compared with the analytical solutions presented by Hull. It is shown that Hull's solution was partially incorrect because the number of modes was not chosen correctly.

Although much attention has been devoted to the modeling of anechoic coatings, the prediction of absorptive performance of a fluid-loaded acoustic coating affixed to a rib-stiffened plate in three dimensions has not been reported in the literatures. In this study, the sound absorption of anechoic coatings embedded with doubly periodic cavities and backed with periodically rib-stiffened plates is therefore investigated. The problem is solved by writing a finite element program using Bloch periodic boundary condition in three dimensions, and the mesh data are exported from ANSYS. Numerical results given by the proposed method are compared with those of a simplified transfer impedance model to reveal the physical mechanism involved.

II. THEORETICAL FORMULATION

The structure consisting of an anechoic coating and a rib-stiffened backing plate is illustrated in Fig. 1. The anechoic coating is made up of viscoelastic materials embedded with air cavities and water-loaded at one side. It is assumed to be infinite in the x and y directions, so the fluid loading on the side of the anechoic coating is semi-infinite. The fluid medium below the backing plate is air and its influence is neglected. The cavities are periodically arranged at a distance of a in the x direction and b in the y directions, respectively. The ribs attached to the plate are equally spaced at a distance of L in the x direction and usually L is

[a)]Author to whom correspondence should be addressed. Electronic mail: liubl@mail.ioa.ac.cn

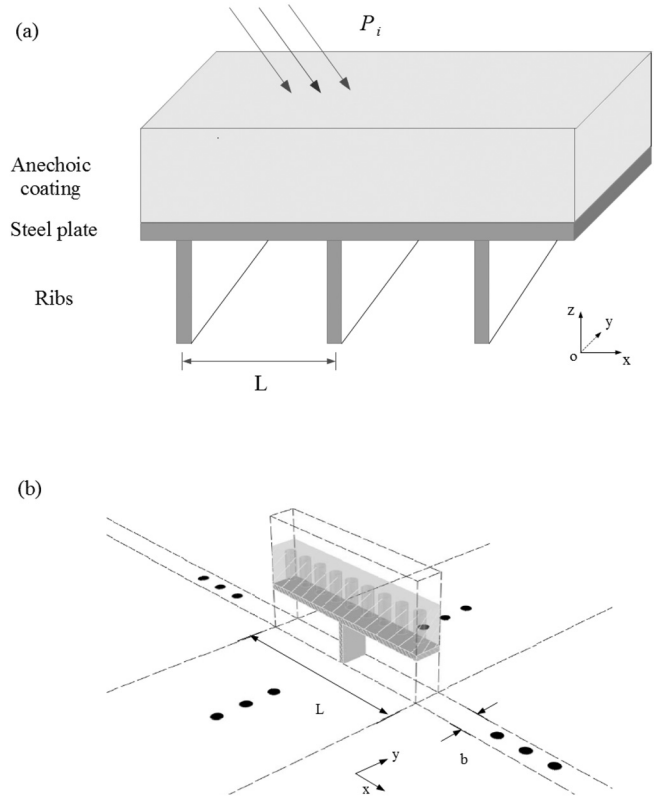

FIG. 1. (a) Schematic description of a rib-stiffened plate covered with an anechoic coating. (b) One unit cell to be meshed for FEM calculation.

several times of a. Therefore a sub area with the periodic distances L in the x direction and b in the y direction can be regarded as a unit cell of the structure. When the unit cell for periodic expansion is determined, following the approach given by Hennion,[10,11] the reflection and transmission coefficients can be calculated by FEM.

The structure is excited by a harmonic plane wave from the semi-infinite fluid medium. The expression of the incident wave is

$$p_i(x,y,z) = \exp[-jk(x\sin\theta\cos\varphi + y\sin\theta\sin\varphi + z\cos\theta)], \tag{1}$$

where the time dependence $e^{-j\omega t}$ has been omitted for clarity, θ and φ indicate the direction of wave incidence, k and ω are, respectively, the wave number and the angular frequency in the fluid.

According to Bloch's theorem, if the structure has the periodic distance L in the x direction and b in the y direction, any space function x (such as displacement and pressure) satisfies the following relation:[11]

$$\chi(\mathrm{x}+L,\mathrm{y}+b,\mathrm{z}) = \chi(\mathrm{x},\mathrm{y},\mathrm{z})e^{jLk\sin\theta\cos\varphi}e^{jbk\sin\theta\sin\varphi}, \tag{2}$$

which indicates a phase relation between nodes separated by one period.

Using this relation, the reflected and transmitted waves can be represented as doubly infinite series of the waves radiated or scattered by the structure. In these expansions, the high-order elementary waves are evanescent, so it is reasonable to take a finite series, as in the following text:

$$p_r(x,y) = \sum_{n=-N_x}^{N_x}\sum_{m=-M_y}^{M_y} R_{nm}e^{-j(k_{nx}x+k_{my}y-k_{nm}z)}, \tag{3}$$

$$p_t(x,y) = \sum_{n=-N_x}^{N_x}\sum_{m=-M_y}^{M_y} T_{nm}e^{-j(k_{nx}x+k_{my}y+k_{nm}z)}, \tag{4}$$

where

$$k_{nx} = n\pi/2L + k\sin\theta\cos\varphi, \tag{5}$$

$$k_{my} = m\pi/2b + k\sin\theta\sin\varphi, \tag{6}$$

$$k_{nm}^2 = k^2 - k_{nx}^2 - k_{my}^2, \tag{7}$$

and R_{nm} and T_{nm} are the reflection coefficient and transmission coefficient corresponding to the (m,n)th mode.

Due to the use of the Bloch relations [Eq. (2)], only one unit cell of the periodic structure, including a small part of the fluid domain, has to be meshed. The unit cell can be divided into nine parts including four surfaces S_1, S_2, S_3, S_4, four corner lines C_1, C_2, C_3, C_4, and the inner domain, as shown in Fig. 2.

Because the structure is fluid-loaded on the side of the anechoic coating, the coupling effect of the fluid and structure must be taken into account. The Bloch relations [Eq. (2)] provide boundary conditions between adjacent cells. By using the Galerkin method, the discrete equations of the FEM for the fluid-structure interaction problem can be written in the assembled form as

$$\begin{bmatrix} -\boldsymbol{R}^T & \boldsymbol{K_s} - \omega^2\boldsymbol{M_s} \\ \boldsymbol{K_f} - \omega^2\boldsymbol{M_f} & -\rho_0\omega^2\boldsymbol{R} \end{bmatrix} \begin{Bmatrix} \boldsymbol{p} \\ \boldsymbol{\delta} \end{Bmatrix} = \begin{Bmatrix} \boldsymbol{F_m} \\ \boldsymbol{\Phi} \end{Bmatrix}, \tag{8}$$

where the unknowns are the vectors of nodal values of the pressure $\boldsymbol{p}$ and of the displacement $\boldsymbol{\delta}$, $\boldsymbol{M_f}$, $\boldsymbol{K_f}$ are the fluid mass matrix and fluid stiffness matrix, while $\boldsymbol{M_s}$ and $\boldsymbol{K_s}$ are the mass matrix and stiffness matrix for the structure, $\boldsymbol{R}$ is the matrix that describes the coupling effect between the structure and the fluid, $\boldsymbol{F_m}$ contains the nodal values of the applied forces, $\boldsymbol{\Phi}$ contains the nodal values of the pressure normal gradient on the fluid domain boundary, ρ_0 is the fluid density, ω denotes the angular frequency.

By solving the Eq. (8), the nodal values of the pressure on the incident surface and transmission surface, known as p_- and p_+, can be obtained. p_- and p_+ have the relations

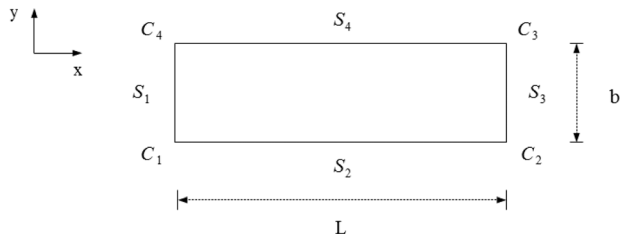

FIG. 2. Cross-sectional view of a unit cell.

$$p_- = p_i + p_r, \tag{9}$$

$$p_+ = p_t. \tag{10}$$

The first term in Eq. (9) is the incident wave given by Eq. (1), and the second term is the reflected wave given by Eq. (3). By subtracting the incident wave from p_-, the nodal values of the reflected pressure on the incident surface can be acquired. Because the unknowns R_{nm} and T_{nm} have $N = (2N_x+1)(2M_y+1)$ terms, by taking N nodal pressure values from the incident surface and transmission surface, two sets of equations can be established. Then R_{nm} and T_{nm} can be obtained, and the reflection coefficient and transmission coefficient can also be derived as

$$R = \frac{\sqrt{\sum_{N_x}\sum_{M_y}|R_{nm}|^2}}{N}, \tag{11}$$

$$T = \frac{\sqrt{\sum_{N_x}\sum_{M_y}|T_{nm}|^2}}{N}. \tag{12}$$

The absorption coefficient can then be calculated from the following equation:

$$\alpha = 1 - R^2 - T^2. \tag{13}$$

III. ANALYSIS ON SOUND ABSORPTION PERFORMANCE

In analysis, hexahedral elements are used to mesh the structural and fluid domain. The mesh size follows that a $\lambda/12$ criterion is applied on the shear waves and a $\lambda/4$ criterion on the flexural waves. Using the mesh data exported from ANSYS, a finite element program based on MATLAB environment has been developed. In this section, the verification of the FEM program is presented at the beginning, and then the FEM program is applied to solve a typically coated structure illustrated in Fig. 1.

A. Verification of the FEM program developed

To verify the FEM program, the absorption coefficients of a plate coated with a homogeneous elastic layer are calculated by the FEM program and transfer matrix method for a comparison as illustrated in Fig. 3. The homogeneous coating layer has a thickness of 5 cm and the plate 1.2 cm. The Young's modulus of the coating layer is assumed as 1.4e8 Pa and frequency independence, the loss factor is 0.23, the density 1100 kg/m^3, and Poisson ratio 0.49. The Young's modulus, density, and Poisson's ratio of the steel plate are 2.16e11 Pa, 7800 kg/m^3, and 0.3, respectively. The thickness of the fluid domain is set 10 cm for which the evanescent wave decays sufficiently in the frequency range of calculation. The density and sound speed of the fluid are assumed to be 1000 kg/m^3 and 1500 m/s. The coating does not contain any air cavities and is assumed to be infinite in the x and y directions. Theoretically the results calculated by those two

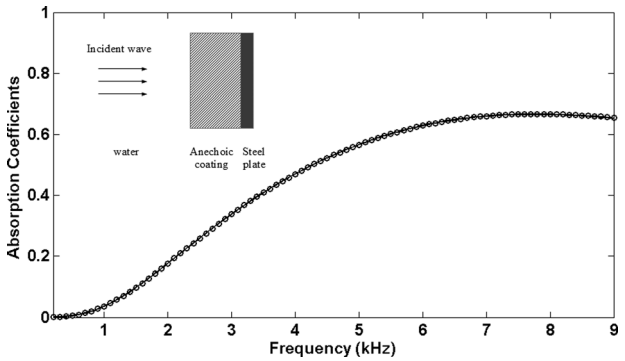

FIG. 3. Comparison of absorption coefficients calculated by FEM program and transfer matrix method. Solid line, FEM program; dashed line, transfer matrix method.

methods should agree with each other, and this is verified in Fig. 3; the agreement provides a validation of the FEM program developed.

Another example is illustrated in Fig. 4 for a coating layer embedded with air cavities. The parameters used in this example are the same as those described in Ref. 15, where the thickness of coating layer is 4 cm and the embedded cylindrical cavity has a height of 2 cm and radius of 1 cm. The Young modulus is 1.4e8 Pa, the loss factor 0.23, the density 1100 kg/m^3, and Poisson ratio 0.49. In Fig. 4, the solid, dashed and dashed-dotted lines denote the reflection coefficients calculated by the FEM program in which the unit cells meshed for calculation contain respectively one, two, and five air cavities, while the circle line denotes the results reproduced from Ref. 15. The results imply that the unit cell length adopted for the FEM mesh is not sensitive to the calculation results, and all curves are well agreed with that in Ref. 15.

B. Sound absorption of a coated and rib-stiffened plate under normal incident waves

Sound absorption of the coated and rib-stiffened plate under normal incident waves was investigated in this part. In the calculation, the thickness of the coating layer is assumed as 4.2 cm and the steel plate 1.2 cm. The embedded air cavity has cylindrical shape with a diameter of 1.2 cm and a height of 3 cm. The distance between two cavities is 3 cm.

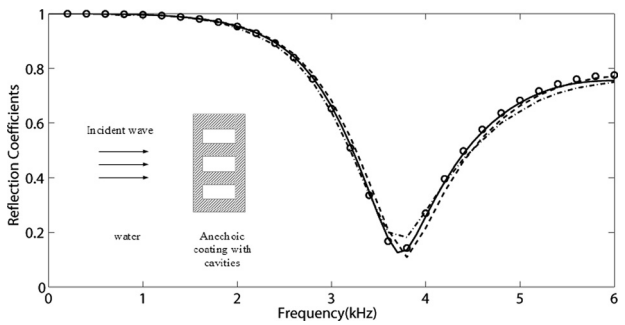

FIG. 4. Comparison of predicted reflection coefficients. Circle, reproduced from Ref. 15; solid line, current program where the unit cell contains one air cavity; dashed line, contains two cavities; dashed-dotted line, contains five cavities.

The ribs attached to the steel plate are 0.8 cm in width and 15 cm in height. The distance between two ribs is 30 cm, therefore one period of the ribbed-plate in the length direction is 30 cm, and each period contains ten air cavities of the coating layer. The Young's modulus, density, Poisson ratio, and loss factor of the coating material are assumed as 2.5e7 Pa, 1100 kg/m^3, 0.49, and 0.23, respectively. The nodes for one unit cell are about 4.8e4, and the calculation time for 80 frequency points is about 100 h by using a HP Workstation Z800.

The predicted absorption coefficients are shown in Fig. 5, where the dashed line represents the results of the coating layer without steel plate attachments, the solid curve denotes that of the coating layer attached to the steel plate, and the dashed-dotted curve denotes that of the coating layer attached to the rib-stiffened steel plate. It is interesting to note that all of three curves have absorption peaks, and in comparison with the coating layer, the main absorption peak moves to the lower frequency range significantly as the steel plate and the ribs are enclosed. For the case studied, the main absorption peak of the coating layer is located around 2000 Hz, this peak shifts to 850 Hz when the plate is enclosed and to 700 Hz when the ribs are attached.

The main reason that results in the shifting of the absorption peak is due to the increased mass of the plate and the ribs. If we consider an equivalent homogeneous layer and assume that its input impedance is equal to that of the calculated coating layer with air cavities included, then the input impedance may be expressed by[16]

$$Z_0 = j\rho_e c_e \tan k_e l, \tag{14}$$

where ρ_e and c_e are the equivalent density and the equivalent wave speed of the coating layer, respectively, $k_e = \omega/c_e$ is the equivalent wavenumber, and l is the thickness of the coating layer.

When the equivalent rubber layer is affixed to a plate, the corresponding input impedance, according to the well-known impedance transfer formula,[16] is given by

$$Z_0^p = \rho_e c_e \frac{Z_p + j\rho_e c_e \tan k_e l}{\rho_e c_e - jZ_p \tan k_e l}, \tag{15}$$

where $Z_p = jm_p\omega$ is the impedance of the plate due to the increased mass per unit area m_p. Similarly for the ribbed plates, the increased mass is taken by $m_p + m_r$, where m_r is the mass increased per unit area due to the ribs. Equation (15) implies that the impedance of the plate with an equivalent homogeneous layer can be determined easily provided that ρ_e and c_e are given.

For the case studied, ρ_e can be easily estimated as 1001 kg/m^3, while the complex number c_e is solved by Monte Carlo iterative method[17] according to the nonlinear Eq. (14) provided that the initial value of c_e is preset and the input impedance Z_0 is known. It should be noted that Z_0 is calculated according to reflection coefficient R_{00}. For the frequencies of interest the evanescent wave decays sufficiently at normal incidence, only plane wave exists in the truncation surface of fluid domain, therefore R in Eq. (11) is equal to R_{00} in calculation. Because $Z_0 = (1+R)/(1-R)$, when the reflection coefficient R is close to 1, a small error in R calculation will result in larger discrepancy in the estimation of Z_0 and therefore in c_e as well; to avoid this deficiency, c_e is estimated according to Eqs. (11) and (14) when R is close to minimum, as

$$c_e = 325(1 + 0.11j), \tag{16}$$

and c_e is further assumed to be independent with frequency when calculate the input impedance in terms of Eq. (15).

When the input impedance is determined, the reflection coefficients and absorption coefficients of coated plate can be easily calculated. An example of this approach is illustrated in Fig. 6, where the predicted absorption coefficients of coating layers with and without the plate and ribs are given for a comparison. Similar to that of Fig. 5, it is evident that the absorption peak shifts to the lower frequency range significantly as the plate and ribs are enclosed. The main absorption peak of the coating layer at 2000 Hz shifts to 850 Hz when the plate is enclosed and to 700 Hz when the

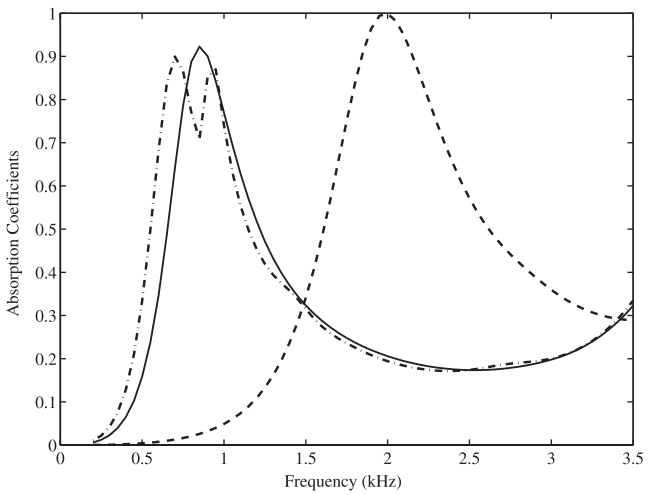

FIG. 5. Predicted absorption coefficients of the coated and rib-stiffened plate under normal incident waves. Dashed line, coating layer; solid line, coating layer attached to the steel plate; dashed-dotted line, coating layer attached to the rib-stiffened plate.

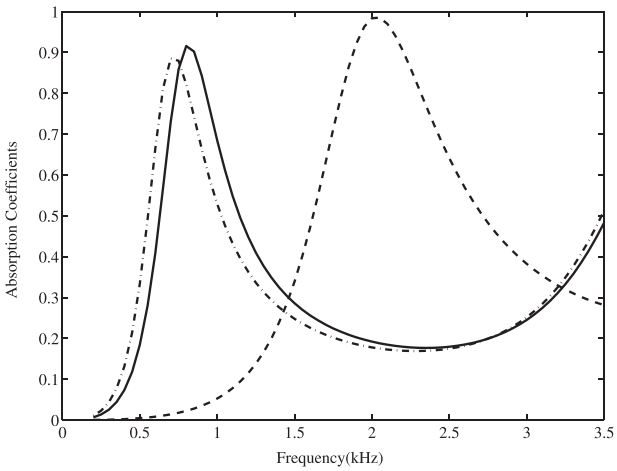

FIG. 6. Predicted absorption coefficients of the coated and rib-stiffened structure using the equivalent impedance transfer formula. Dashed line, coating layer; solid line, coating layer attached to the steel plate; dashed-dotted line, coating layer attached to the rib-stiffened plate.

ribs are attached. These results confirm that the increased mass resulting from the plate and ribs is essential for the sound absorption in the lower frequencies.

Although the increased mass assumption based on Eq. (15) is able to explain the main absorption peak around 700 Hz when ribs attached, in comparison with Fig. 5, one should note that this assumption is not able to predict the additional peak around 900 Hz. The assumption is valid only when the plate and the ribs move in phase. If the ribs and the plate do not move in phase, the assumption has no longer effective. The other discrepancy appears above 3 kHz, and this might be due to the assumption that the wave speed is independent on frequency in Eq. (16). When frequency goes higher, or roughly saying above the half wavelength of the longitudinal wave of the equivalent coating layer, the coupling between the coating and the ribbed plate becomes complicated and that makes the assumption no longer effective.

The approach also implies that the prediction of main absorption performances of the coated structures may be simplified by two steps. (1) One may use FEM to calculate the input impedance of the coating layer. The coating layer is embedded with air cavities and water-loaded at one side and air-occupied at other side. Then one can employ the input impedance of coating layer to obtain equivalent wave speed or equivalent elastic modulus for an equivalent coating layer. At this step, only the coating layer is considered, and the unit cell to be meshed contains only one air cavity. In comparison with that of the coated and ribbed plate, the mesh size is much less, and the calculation time is reduced significantly. (2) One may calculate the equivalent coating layer affixed to a periodically rib-stiffened plates or even more complicated structures by FEM. At this step, only the equivalent homogeneous layer is considered, and therefore larger mesh size is applicable to save the calculation time. The predicted results given by simplified approach and non-simplified approach are illustrated in Fig. 7. The two curves agree with each other in the frequencies of the main absorption range. While the calculation time run by the simplified approach is only about 1/30 of non- simplified approach.

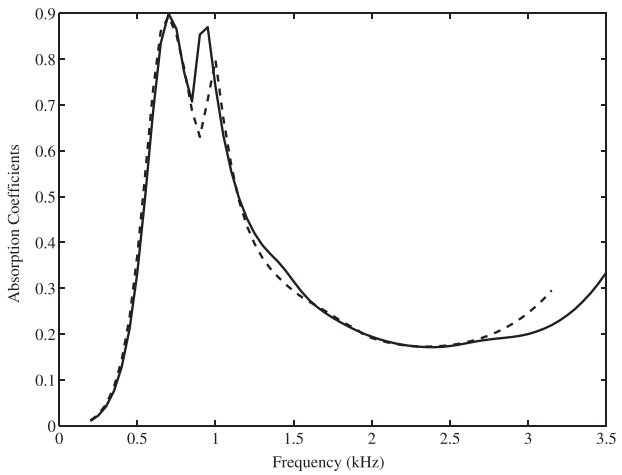

FIG. 7. Predicted absorption coefficients of a coated and rib-stiffened structure by FEM. Solid line, the unit cell meshed for calculation includes ten air cavities; dashed line, simplified approach using an equivalent coating layer.

IV. CONCLUSIONS

Sound absorption of anechoic coating embedded with periodic cavities and backed with periodically rib-stiffened plates is investigated by using the FEM combined with Bloch-periodic boundary conditions. A simplified approach based on the FEM and transfer impedance model is also introduced for a comparison. The results indicate that the increased mass resulting from the plate and ribs is essential for the sound absorption in the lower frequencies. The shifting of the absorption peak could reach to one or two octave band depending on the increased mass of backing plates, and this is valuable for these efforts to achieve sound absorption especially in low frequency range.

The results also imply that the prediction of the main absorption performance of coated structures may be simplified by calculating an equivalent homogeneous coating layer affixed to the periodically rib-stiffened plate or even more complicated structures by the FEM. This approach helps to catch the main absorption performance while at the same time reduce the calculation time dramatically in comparison with a full FEM model.

ACKNOWLEDGMENTS

The authors gratefully acknowledge the financial support from NSFC Grant No. 11374326 and State Key Development Program for Basic Research of China (973 Program) Grant No. 2012CB720204.

[1]J. S. Sastry and M. L. Munjal, "A transfer matrix approach for evaluation of the response of a multi-layer infinite plate to a two-dimensional pressure excitation," J. Sound Vib. **182**, 109–128 (1995).
[2]G. C. Gaunaurd and W. Wertman, "Comparison of effective medium theories for inhomogeneous continua," J. Acoust. Soc. Am. **85**, 541–554 (1989).
[3]G. C. Gaunaurd and H. Überall, "Resonance theory of the effective properties of perforated solids," J. Acoust. Soc. Am. **71**, 282–295 (1982).
[4]G. C. Gaunaurd and H. Überall, "Theory of resonant scattering from spherical cavities in elastic and viscoelastic media," J. Acoust. Soc. Am. **63**, 1699–1712 (1978).
[5]D. Bai and J. B. Keller, "Sound waves in a periodic medium containing rigid spheres," J. Acoust. Soc. Am. **82**, 1436–1441 (1987).
[6]S. M. Ivansson, "Anechoic coatings obtained from two-and three-dimensional monopole resonance diffraction gratings," J. Acoust. Soc. Am. **131**, 2622–2637 (2012).
[7]S. M. Ivansson, "Numerical design of Alberich anechoic coatings with superellipsoidal cavities of mixed sizes," J. Acoust. Soc. Am. **124**, 1974–1984 (2008).
[8]S. M. Ivansson, "Sound absorption by viscoelastic coatings with periodically distributed cavities," J. Acoust. Soc. Am. **119**, 3558–3567 (2006).
[9]G. C. Gaunaurd, "One-dimensional model for acoustic absorption in a viscoelastic medium containing short cylindrical cavities," J. Acoust. Soc. Am. **62**, 298–307 (1977).
[10]A. C. Hennion, R. Bossut, J. N. Decarpigny, and C. Audoly, "Analysis of the scattering of a plane acoustic wave by a periodic elastic structure using the finite element method: Application to compliant tube gratings," J. Acoust. Soc. Am. **87**, 1861–1870 (1990).
[11]A. C. Hennion and J. N. Decarpigny, "Analysis of the scattering of a plane acoustic wave by a doubly periodic structure using the finite element method: Application to Alberich anechoic coatings," J. Acoust. Soc. Am. **90**, 3356–3367 (1991).
[12]H. Meng, J. H. Wen, H. G. Zhao, L. M. Lv, and X. S. Wen, "Analysis of absorption performances of anechoic layers with steel plate backing," J. Acoust. Soc. Am. **132**, 69–75 (2012).
[13]A. J. Hull and J. R. Welch, "Elastic response of an acoustic coating on a rib-stiffened plate," J. Sound Vib. **329**, 4192–4211 (2010).

[14]M. C. Remillieux and R. A. Burdisso, "Vibro-acoustic response of an infinite, rib-stiffened, thick-plate assembly using finite-element analysis," J. Acoust. Soc. Am. **132**, EL36–EL42 (2012).
[15]M. Wang, "Theoretical and experimental research on underwater anechoic coating," Ph.D. thesis, Harbin Engineering University, China, 2004 (in Chinese).
[16]J. Allard and N. Atalla, *Propagation of Sound in Porous Media: Modelling Sound Absorbing Materials*, 2nd ed. (Wiley and Sons, London, 2009), Chap. 2.
[17]J. C. Walter and G. T. Barkema, "An introduction to Monte Carlo methods," Phys. A **418**, 78–87 (2015).